



SH31A-2528 Interstellar He Flow Analysis over the Past 8 Years with IBEX Neutral Observations

E. Möbius¹, E. Bower¹, M. Bzowski², S.A. Fuselier^{3,4}, D. Heitzler¹, M.A. Kubiak², H. Kucharek¹, M.A. Lee¹

T. Leonard⁵, D.J. McComas^{6,7}, N. Schwadron¹, P. Swaczyna², J.M. Sokol², P. Würz⁸

Contact: eberhard.moebius@unh.edu



Supported by:
NASA USA
PAS Poland
SNF Switzerland

¹Space Science Center & Department of Physics, University of New Hampshire, Durham, NH 03824

²Space Research Center Polish Academy of Sciences, Warszawa, Poland

³Southwest Research Institute, San Antonio, TX

⁴University of Texas, San Antonio, TX

⁵Laboratory for Atmospheric and Space Physics, Boulder, CO

⁶Department of Astrophysical Sciences, Princeton University, NJ

⁷Office of the VP for the Princeton PPL, Princeton University, NJ

⁸Physikalisches Institut, Universität Bern, Switzerland

Introduction

The Interstellar Boundary Explorer (IBEX) obtains a precise relation between the interstellar neutral (ISN) flow longitude $\lambda_{ISN\infty}$ and speed $V_{ISN\infty}$ with substantially larger uncertainty in $\lambda_{ISN\infty}$, which defines a parameter tube that connects ISN longitude, latitude, speed (velocity vector $V_{ISN\infty}$), and temperature [1, 2, 3, 4, 5], in agreement with Ulysses GAS [6, 7, 8] (Figure 1). The interstellar magnetic field B_{IS} is deduced from the IBEX ribbon, consistent with the heliospheric asymmetry and TeV cosmic ray anisotropy [9]. The two vectors define the B_{IS} - $V_{ISN\infty}$ plane, which controls the shape of, and the flow deflection in, the outer heliosheath [10, 11]. A complementary determination of $\lambda_{ISN\infty}$ (Poster SH31A-2529) together with tightening and tracking over time the parameter tube will refine the B_{IS} - $V_{ISN\infty}$ plane and constrain any potential temporal variations [12, 13, 14].

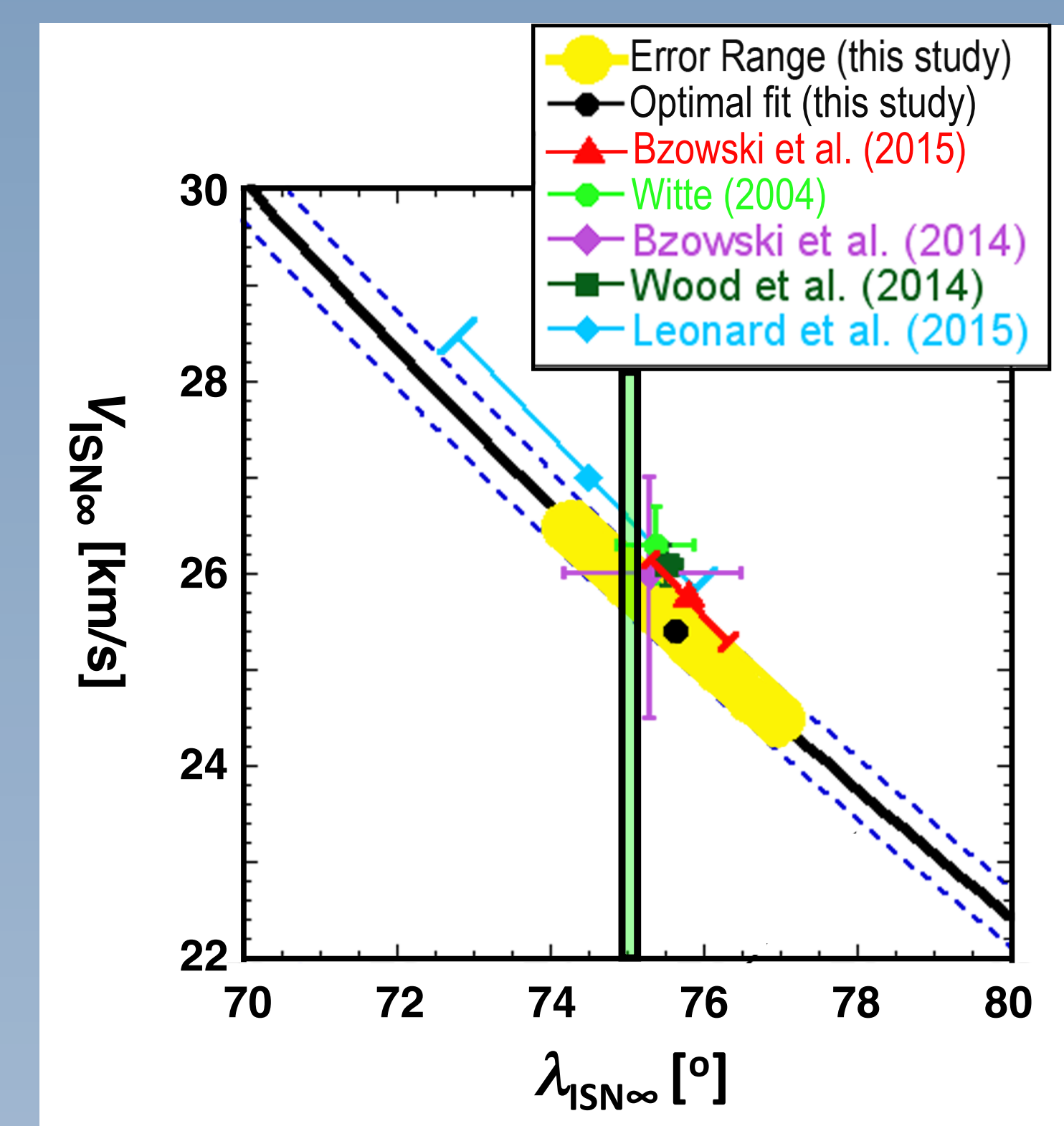


FIGURE 1: Relationship between $V_{ISN\infty}$ and $\lambda_{ISN\infty}$ according to the IBEX parameter tube based on various IBEX analyses in comparison with Ulysses results (adapted from [5]). Also shown with a vertical bar is how an independent measurement of $\lambda_{ISN\infty}$ will constrain the ISN flow vector. The effect of a precise independent determination of the ISN flow longitude $\lambda_{ISN\infty}$ on the knowledge of the ISN flow parameters is indicated by the green vertical bar.

ISN Parameter Tube and Flow Longitude

• **ISN Parameter Tube Determination:** The parameter tube is solely determined by the ISN bulk flow (ISN flow maximum) longitude $\lambda_{ISN\text{Peak}}$ at 1 AU observed with IBEX [4, 15] (discussed on this Poster).

• **Flow Longitude Determination:** The ISN flow longitude $\lambda_{ISN\infty}$ is determined from the variation of the radial ISN flow speed V_r (or the pickup ion cut-off along the Earth's orbit, which is symmetric about $\lambda_{ISN\infty}$) (discussed on Poster SH31A-2529).

$$2) v_r^2 = 2 + v_{ISN\infty}^2 - (1 - \cos \lambda) - \left\{ \frac{v_{ISN\infty}^2 \sin^2 \lambda + v_{ISN\infty} \sin |\lambda| \cdot \left[v_{ISN\infty}^2 \sin^2 \lambda + 4(1 - \cos \lambda) \right]^{1/2}}{2} \right\}$$

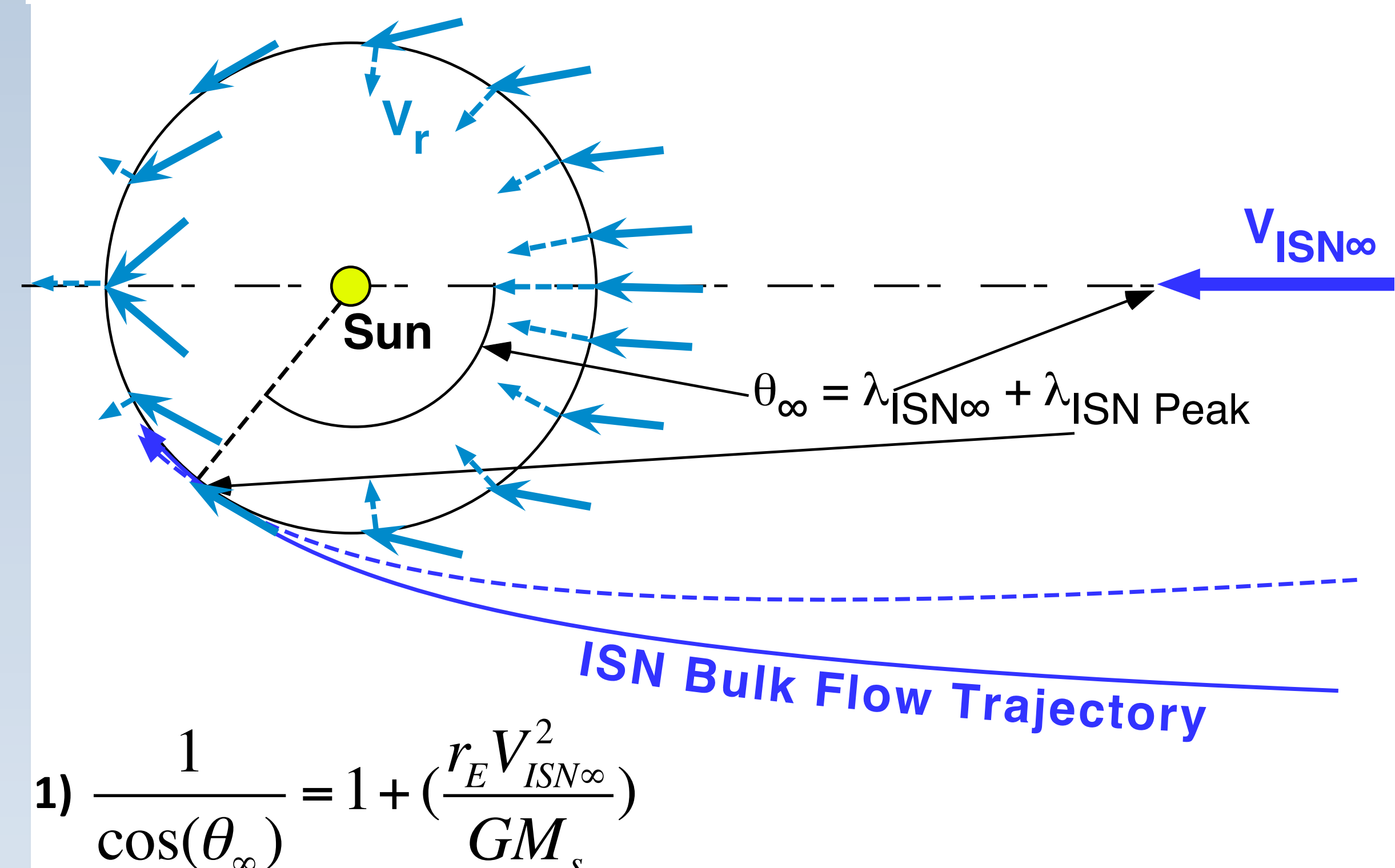


FIGURE 2: Schematic view of sample ISN trajectories (dark blue) and the ISN flow vector along the Earth's orbit (light blue). The dark blue dashed line indicates an alternate Bulk Flow Trajectory that satisfies eq. 1), arrives at $\lambda_{ISN\text{Peak}}$, and thus also belongs to the ISN parameter tube. The light blue dashed arrows indicate the pattern of V_r , which is sensed by the pickup ion cut-off and follows eq. 2).

Determination of the ISN Flow Peak Longitude

The determination of the the ISN Flow Peak Longitude $\lambda_{ISN\text{Peak}}$ involves the following steps [16]:

- **ISN Good Times** for each IBEX orbit [2], but retain time intervals that are despun at ground because of missing Star Tracker pointing information
- **Spin integrated ISN count rates** $\pm 3\sigma$ of peak divided by σ per 512 spins
- **Linear X^2 fit to these rates** as function of λ_{Ecl} \rightarrow obtain rate at λ_{Ecl} where IBEX spin points exactly at the Sun in λ , adjusted for IBEX motion
- **Compensate rates (see Figure 3) for**
 - Observation of ISN flux, while ISN bulk flow corresponds to peak in Phase Space Density (PSD) of the ISN distribution and Flux $\sim PSD \times V^3$
 - Weakly E-dependent IBEX-Lo efficiency due to variation of ISN energy (E_{ISN}) with λ_{Ecl} (relative in-flight calibration for different IBEX-Lo E-Steps)
 - Extinction by ionization along trajectory in λ_{Ecl} using TIMED & SDO data.

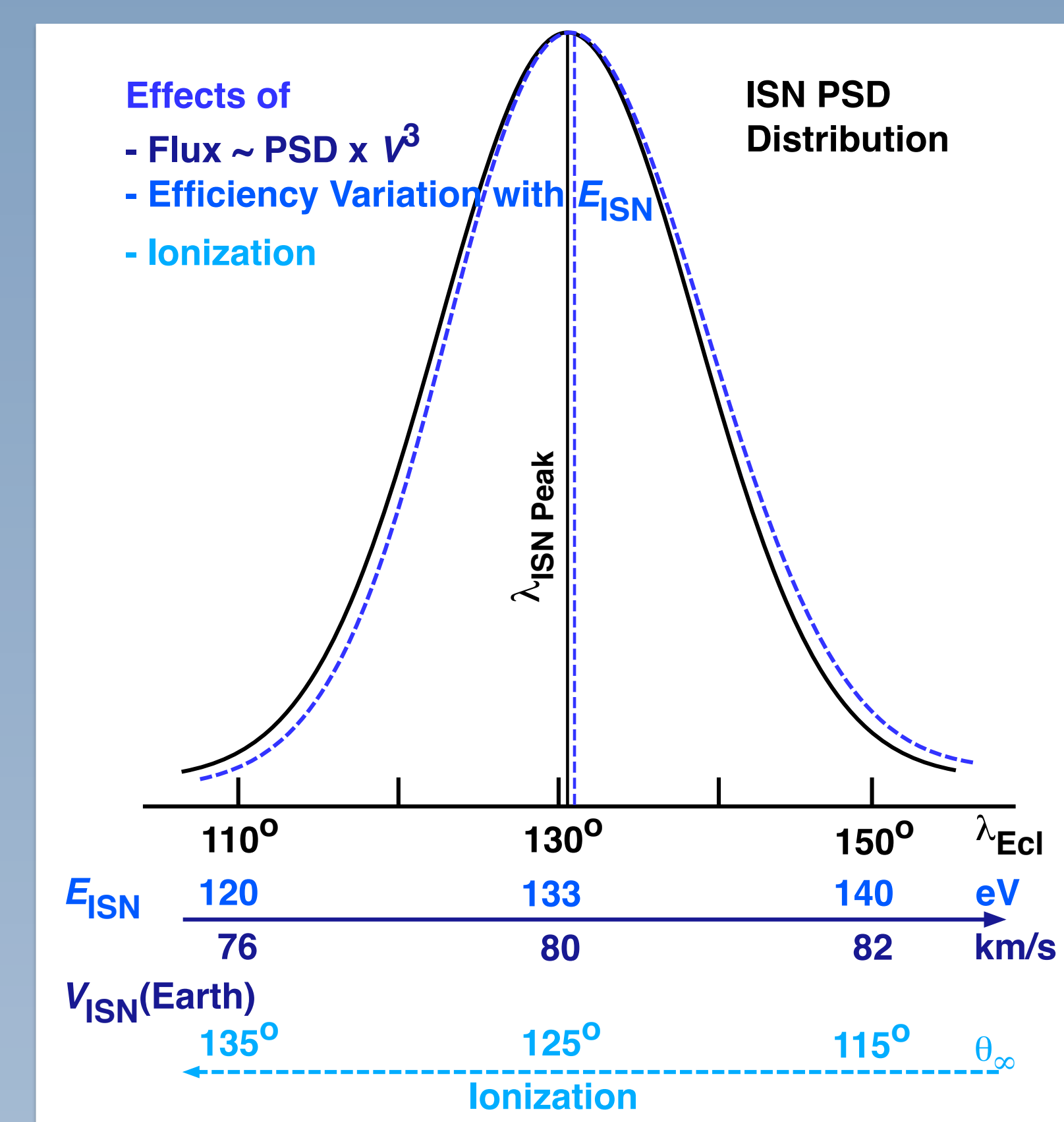


FIGURE 3: ISN PSD distribution (solid black line) as a function of ecliptic longitude λ_{Ecl} . The spin integrated ISN flux (dashed dark blue line) is modified relative to the PSD distribution due to:

- ISN Flux variation with V_{ISN}
- Slight IBEX-Lo Efficiency variation E_{ISN}
- Flux extinction from Ionization

as a function of λ_{Ecl} . To determine $\lambda_{ISN\text{Peak}}$ from the center of the observed flux distribution, these effects have to be compensated for.

Contribution of Secondary He Neutrals: The observed IBEX ISN flux distribution also contains a variable contribution from secondary He neutrals that originate in the outer heliosheath. The ISN distribution is adjusted for the secondary contribution according to Figure 4 [from 17].

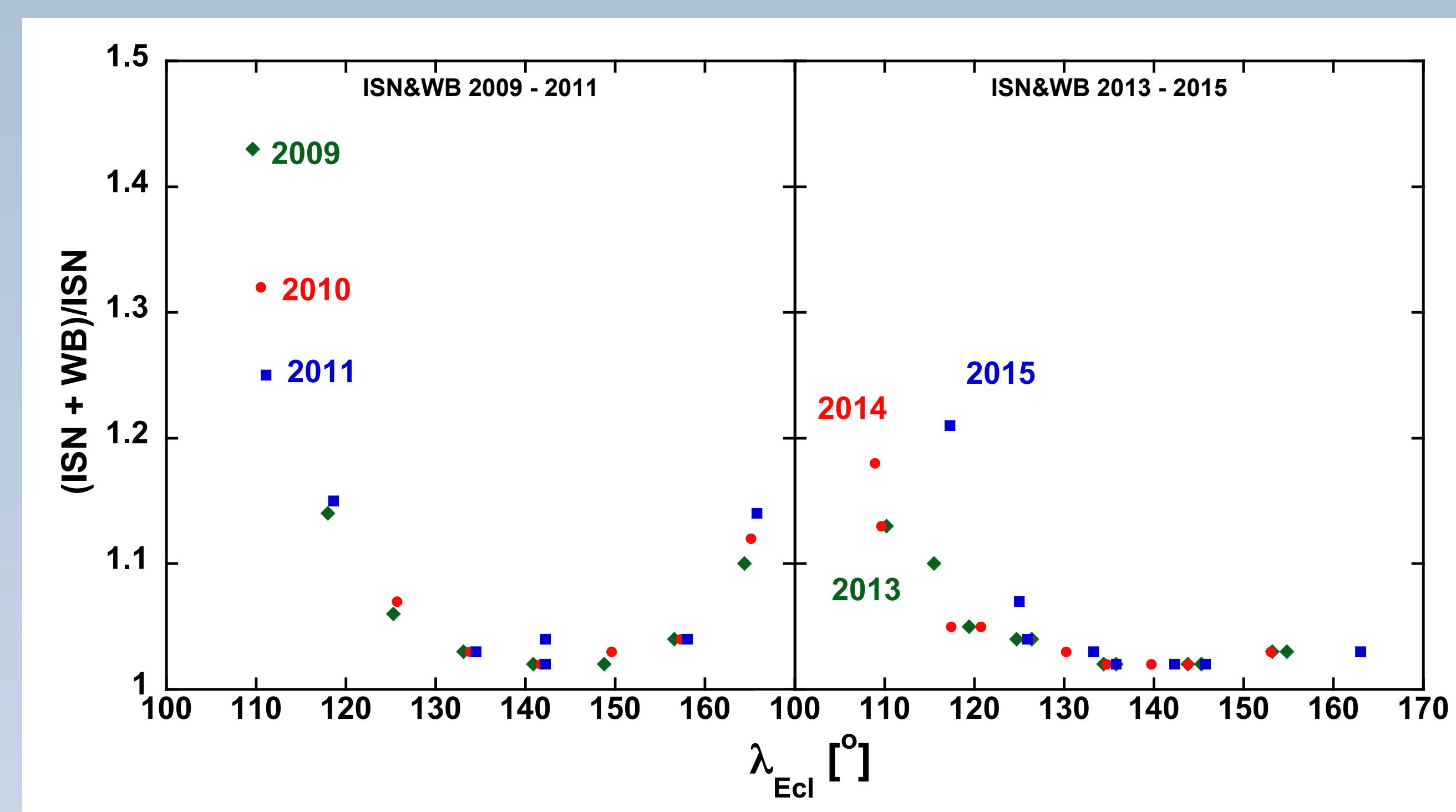


Figure 4: Ratio of combined ISN and secondary He (WB) flux and ISN flux as a function of λ_{Ecl} (by IBEX orbit) obtained from the best fit secondary solution in [17] for 2009 - 11 and 2013 - 15 (2012 not shown because not used here). The relative contribution of the WB is largest at low λ_{Ecl} and during solar minimum (2009-11). The two unusually high points in 2015 are for IBEX spin axis orientations at $+5^\circ$ latitude, indicating increased viewing of the WB for this orientation. The observed ISN fluxes in each orbit are compensated for these ratios.

The Uncertainties of Data for each Orbit contain:

- X^2 -fit error (x2 as fit is restricted to linear and possible curvature omitted)
- uncertainty in adjusting for IBEX motion (translated into the rate, using the slopes of the X^2 -fit and of the model Gaussian in Figure 5)
- uncertainties of the efficiency and ionization compensation

ISN Flow Peak Longitude Fitting

To obtain a value for $\lambda_{ISN\text{Peak}}$ the adjusted rates from each IBEX orbit (or orbit arc after 2011) are evaluated for their variation with λ_{Ecl} . Usable orbits satisfy:

- Observations are within $110^\circ \leq \lambda_{Ecl} \leq 160^\circ$
 - Position at exact Sun pointing of the spin axis is inside of or the extrapolation is less than the range of the data interval in λ_{Ecl}
- These rates are X^2 fitted to a Gaussian for each individual year or the combination of all data after normalizing the rates to the peak rate (as shown in Figure 5).

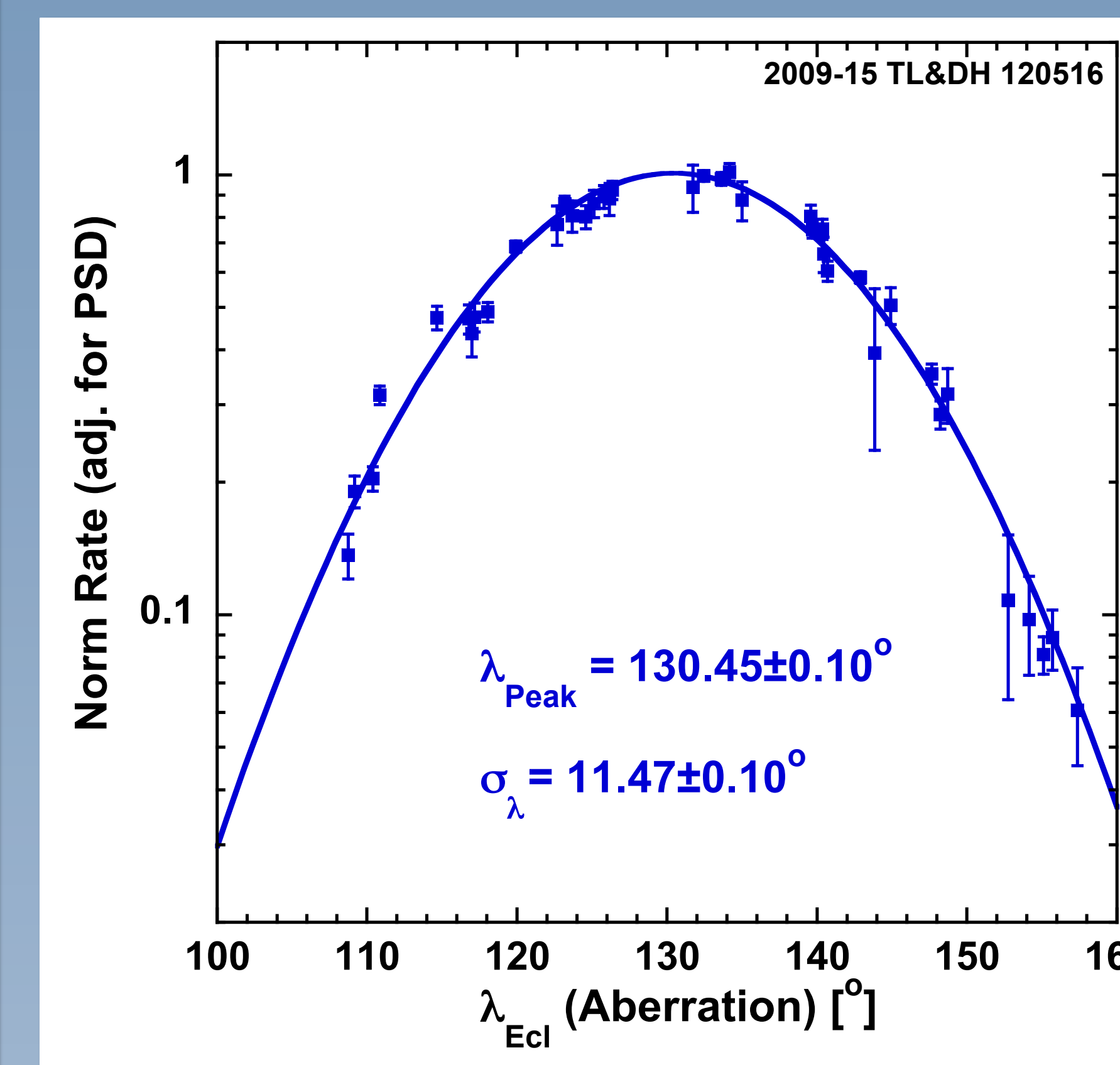


FIGURE 5: ISN fluxes at perihelion for each usable IBEX orbit 2009-15 as a function of λ_{Ecl} adjusted for aberration due to IBEX motion. Error bars contain all known and estimated contributions. Obtained from a X^2 fit to a Gaussian.

Fits to yearly data sets are similar to the combined set in Figure 5, but with larger errors. The yearly fit results are compiled in Figure 6, along with the weighted mean of all yearly fit results and the combined fit result from Figure 5.

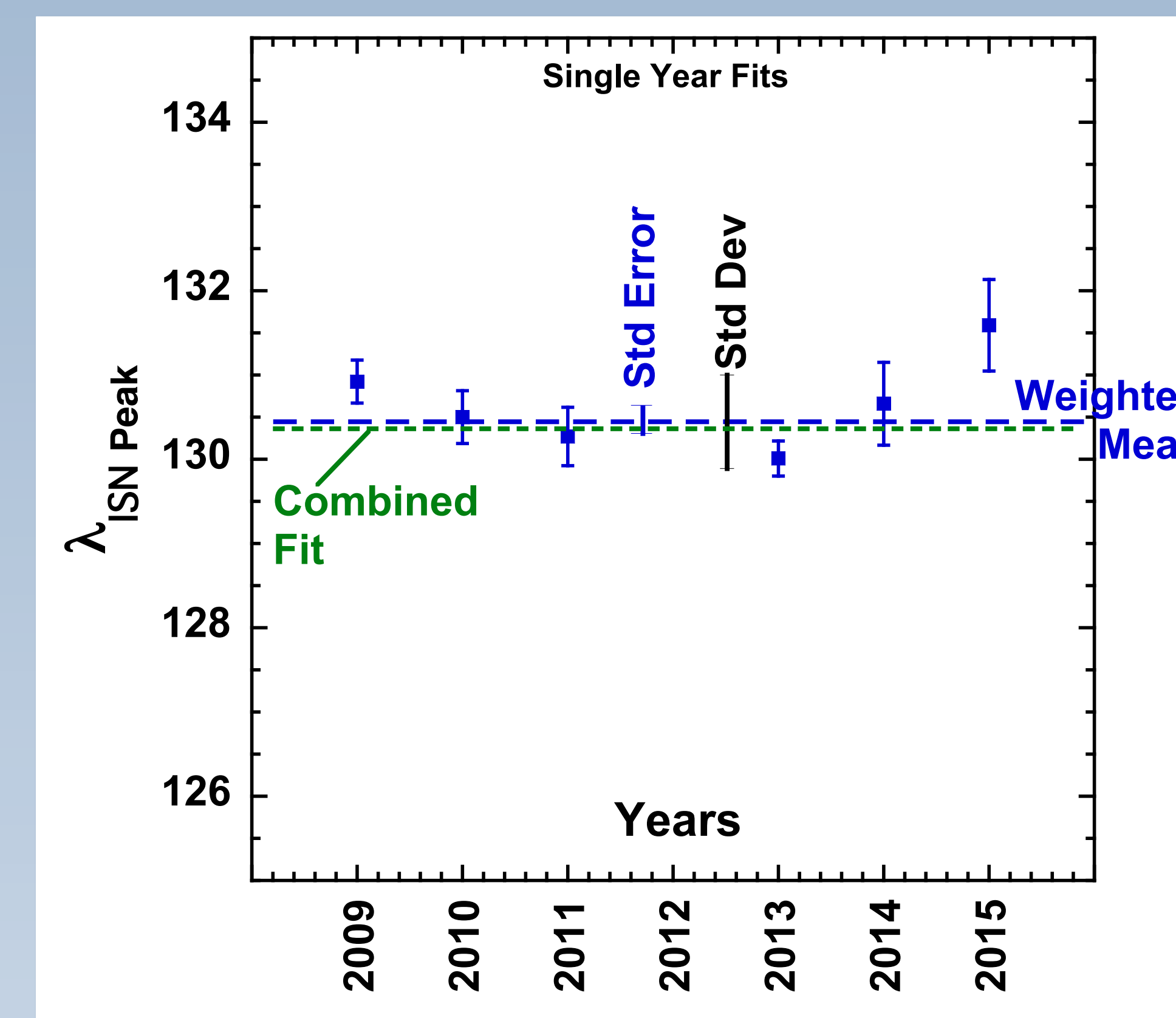


FIGURE 6: $\lambda_{ISN\text{Peak}}$ as obtained from X^2 fits to a Gaussian for the data set of each year, along with the weighted mean, combined fit value from Figure 5, standard deviation and error.

As seen in **Figure 5**, there is no entry for 2012, and the yearly fit values for vary substantially, with 2015 offset by more than 2x the standard deviation.

According to the criteria for usable orbits, the 2012 set only contains 3 data points, not enough for a fit to a Gaussian with 3 free parameters. Thus 2012 was completely omitted.

2015 contains 5 usable orbits over a restricted range in λ_{Ecl} , which by itself does not constrain $\lambda_{ISN\text{Peak}}$ well enough, but can be used in the overall combination. Omitting 2015 from the fit in Figure 5 results in $\lambda_{ISN\text{Peak}} = 130.40 \pm 0.11^\circ$, only different by 0.05° .

ISN Flow Peak Results from Multi-Year Fits

• **Reduction of Systematic Effects with stochastic Distribution:** ISN Good Times influence the results systematically, for example, by forcing extrapolation or data elimination, but they are distributed stochastically each year. Using multi-year data reduces such systematic effects, as demonstrated in [18]. Here we use all 2-year combinations.

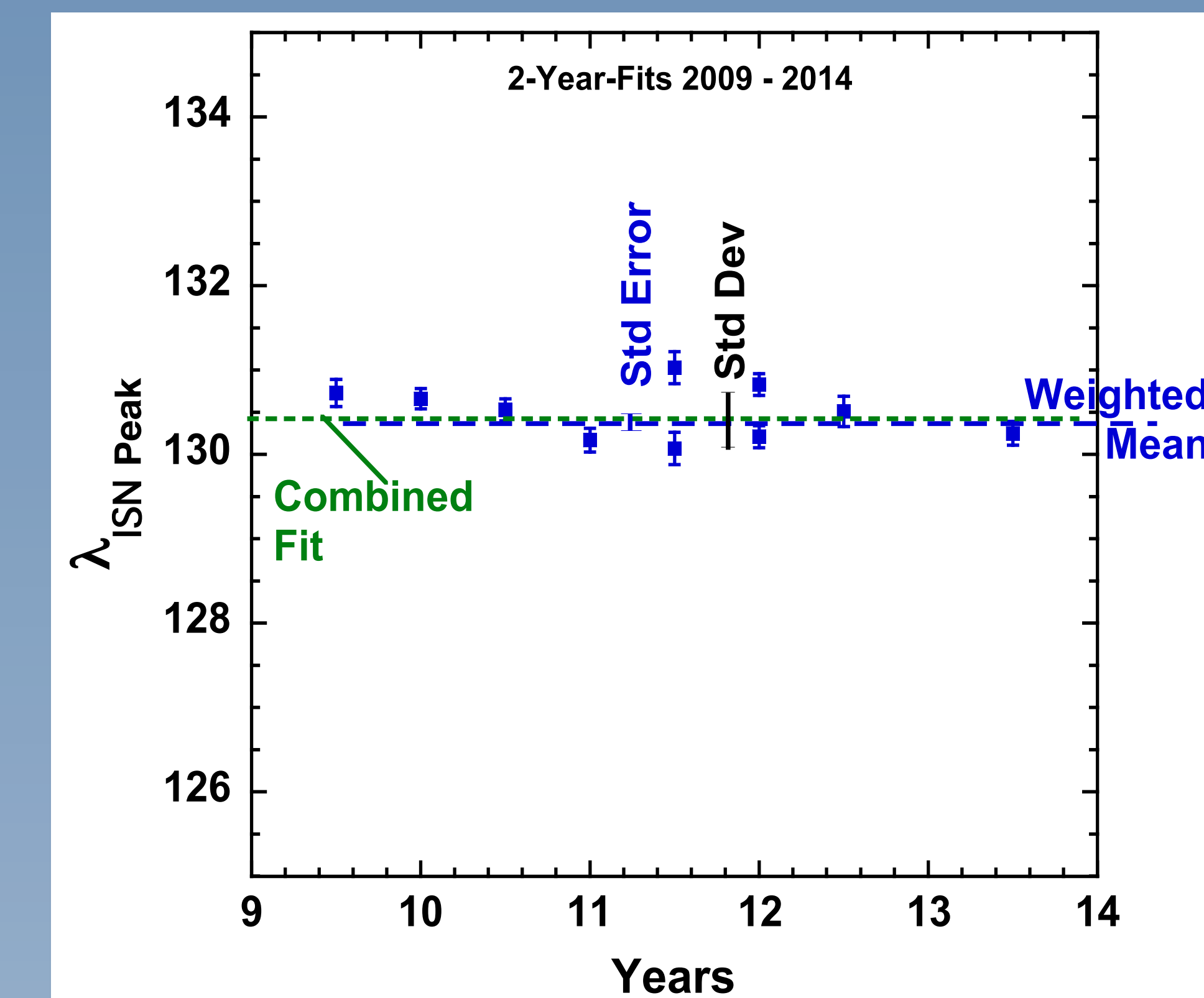


FIGURE 7: $\lambda_{ISN\text{Peak}}$ as obtained from X^2 fits to a Gaussian for data sets of 3-year combinations in all permutations, along with the weighted mean, combined fit value from Figure 5, standard deviation and error.

Figure 7 shows all 2-year combinations sorted by their center time. Combinations with identical center time vary more than those with different times \rightarrow Consistent with no trend! Adding more data points and extending time will reduce uncertainties.

Conclusions & Outlook

• **ISN Flow Peak Longitude:** $\lambda_{ISN\text{Peak}} = 130.45 \pm 0.10^\circ$ from 2009-15 X^2 fit and $\lambda_{ISN\text{Peak}} = 130.45 \pm 0.06^\circ$ from weighted mean of all 2-year (2009-14) fits after adjusting for: **E-dependent efficiency & Secondary Neutrals**

• **ISN Parameter Tube:** Adopting $\lambda_{ISN\infty} = 75.0^\circ$ [3, 5] the parameter tube gives $V_{ISN\infty} = 26.0 \pm 0.1$ km/s, in full agreement with values in [3, 5].

• **Yearly Variations of $\lambda_{ISN\text{Peak}}$:** Yearly values 2009 - 2015 vary with $\pm 0.55^\circ$ Standard Deviation. 2015 strongest deviation, but only 5 usable values \rightarrow eliminated (only 0.05° difference in combined fit)

• **Variation of Sorted 2-Year Fits:** 2-year fits show much reduced variation ($\pm 0.32^\circ$ StdDev) and no visible temporal trend. Weighted mean in full agreement with combined fit results.

Next Steps in Analysis:

- Replace linear fit for each orbit by fit to Analytic Model Results \rightarrow Will increase number of usable orbits
- Add 2016 results after despinning data from operations without IBEX Star Tracker & use IBEX-Lo Energy Steps 1 through 4 \rightarrow Extends existing database

References

1. M. Bzowski et al., *Astrophys. J. Supp.* **220:28** (2015).
2. T. Leonard et al., *Astrophys. J.* **804:42** (2015).
3. D. J. McComas et al., *Astrophys. J. Supp.* **220:22** (2015).
4. E. Möbius et al., *Astrophys. J. Supp.* **220:24** (2015).
5. N.A. Schwadron et al., *Astrophys. J. Supp.* **220:25** (2015).
6. M. Witte, *Astron. & Astrophys.* **426**, 835 (2004).
7. M. Bzowski et al., *Astron. & Astrophys.* **569**, A8 (2014).
8. B. Wood, H.-R. Mueller & M. Witte, *Astrophys. J.* **801:62** (2015).
9. N.A. Schwadron et al., *Science* **343**, 988 (2014).
10. R. Lallement et al., *Science* **307**, 1447 (2005).
11. V. Izmodenov, D. Alexashov & A. Myasnikov, *Astron. & Astrophys.* **437**, L35 (2005).
12. P.C. Frisch et al., *Science* **341**, 1080 (2013).
13. P.C. Frisch et al., *Astrophys. J.* **801:61** (2015).
14. R. Lallement & J.-L. Bertaux, *Astron. & Astrophys.* **565**, A41 (2014).
15. M. A. Lee, E. Möbius & T. Leonard, *Astrophys. J. Supp.* **220:23** (2015).
16. E. Möbius et al., *Astrophys. J. Supp.* **198:11** (2012).
17. M.A. Kubiak et al., *Astrophys. J. Supp.* **223:25** (2016).
18. C. Drews et al., *J. Geophys. Res.* **117**, A09106 (2012).